Bull. Mater. Sci., Vol. 38, No. 1, February 2015, pp. 89–93. © Indian Academy of Sciences.

Effect of Er doping on the superconducting properties of porous MgB_2

O ERDEM[1,2,*] and E YANMAZ[2]

[1]Faculty of Education, Department of Primary Education, Bayburt University, 69000 Bayburt, Turkey
[2]Faculty of Sciences, Department of Physics, Karadeniz Technical University, 61080 Trabzon, Turkey

MS received 21 February 2014; revised 03 May 2014

Abstract. **MgB_2 bulk sample with porous structure was produced by using the *in-situ* solid-state reaction method under argon (Ar) atmosphere of 10 bar. Elemental Er in powder form was doped into MgB_2 with different compositions $(Mg_{1-x}Er_x)B_2$, where $x = 0.00$, 0.03 and 0.05, in order to investigate the effect of rare-earth (RE) element Er on the structural and electromagnetic properties of porous MgB_2. The Er-doped samples result in small grain size structure compared to the undoped one. The lattice constants a and c of the doped samples, determined from X-ray diffraction (XRD) analysis, increase with the increasing Er content, and consequently the superconducting transition temperature (T_c^{onset}) of MgB_2, determined from resistivity measurements, is slightly suppressed. Also, the upper critical field (B_{c2}), the irreversibility field (B_{irr}) and the critical current density (J_c) values are significantly enhanced in the doped samples. For the best sample ($x = 0.03$), at 15 K under a magnetic field of 4 T, the J_c value reaches 2.4×10^4 A cm^{-2}, which is higher than that of the porous sample by an order of 10^3, and the B_{irr} value at 20 K reaches 9.7 T. These results imply that the RE element Er fills the pores, enhances the density and the grain connectivity. Hence, the superconducting properties of the porous MgB_2 sample improve by Er doping.**

Keywords. **Superconductivity; $(Mg_{1-x}Er_x)B_2$; upper critical field; irreversibility field; critical current density.**

1. Introduction

The discovery of superconductivity in MgB_2[1] has stimulated great scientific and technological interest, not only because of its simple electronic structure and high critical temperature (T_c),[1] but also due to its high critical current density (J_c),[2] large coherence length[3] and the absence of weak-link effect.[4]

It is well known that the rapid drop in J_c with the increasing applied magnetic field is one of the major problems for MgB_2-based superconductor technologies. A rapid drop in J_c indicates low irreversibility field (B_{irr}) and poor pinning ability due to a lack of effective pinning centres in MgB_2. The density also has an important effect on the superconducting performance of MgB_2. It is well known that the high occupation fraction of pores in sintered MgB_2 bulk samples decreases the density and the effective cross-section area for carrying current.[5] If the porosity can be decreased and the density can be increased, the critical current density of MgB_2 will be increased significantly. It is well known that the resistivity of dense MgB_2 is smaller than that of porous one.[6] Also, the J_c ($H = 0$) of MgB_2 is inversely proportional to $\Delta\rho$ ($\Delta\rho = \rho(300\text{ K}) - \rho(50\text{ K})$). This follows because the ratio of $\Delta\rho$ in fully dense and clean MgB_2 to $\Delta\rho$ in MgB_2 sample is a measure of the reduction in current-carrying area.[7]

It is possible to improve the pinning behaviour of MgB_2 by many methods, such as adding or doping[8,9] and the introduction of defects by irradiation,[10] etc. Chemical doping is known to be one of the most effective methods in improving the superconducting properties of MgB_2. Doping can substitute dopant atoms for atoms in MgB_2 crystal lattice to increase the upper critical field (B_{c2}) and induce defects and precipitates to increase flux pinning centres of MgB_2.[9,11] However, the results of chemical doping are categorized into two types, as reported by Zhao *et al*:[12] the doping which leads to the decrease of T_c and the loss of superconductivity, such as doping of Al,[13] and the other doping which cannot dope the element in the MgB_2 crystal lattice and has no effect on T_c, such as Be doping.[14] The second type of doping creates non-superconducting phases, which may work as pinning centres if a proper microstructure of the second phases can be formed in MgB_2. It has been reported by Feng *et al*[15] and Zhao *et al* [12] that doping of MgB_2 with Zr and Ti, respectively, increases the sample density, reduces the porosity and increases the J_c values.

Magnetic impurities usually have a stronger interaction with magnetic flux lines than non-magnetic impurities. If the impurities can be properly introduced into the MgB_2 matrix, they may exert a stronger force to trap the flux lines and improve the pinning behaviour of MgB_2. The magnetic doping elements, such as Mn, Fe, Co and Ni, which can depair Cooper pairs, often degrade the superconducting performance of MgB_2 in a magnetic field due to the presence of a local magnetic field.[16–18] On the other hand, rare-earth (RE) elements often possess a strong magnetic moment, however, they do not suppress the superconductivity of MgB_2.[19–21] When RE oxides and elements are doped into MgB_2, they

*Author for correspondence (ozgeerdem@bayburt.edu.tr)

form impurity phases with boron, which can act as effective pinning centres in MgB_2. The main resultants are REB_6 for light REs (La, Ce, Pr, Nd, Sm, Eu, Gd) and REB_4 for heavy RE elements (Tb, Dy, Ho, Er). Also the density of the doped samples increases compared with the undoped one.[22] Doping with RE oxides Pr_6O_{11} and Eu_2O_3 provides strong flux pinning due to the PrB_6 and EuB_6 impurity phases and increases $J_c(H)$, H_{c2} and H_{irr} of MgB_2. J_c values at 10 K under a field of 5 T for undoped ($x = 0.00$), Pr_6O_{11}-doped ($x = 0.03$) and Eu_2O_3-doped ($x = 0.05$) MgB_2 samples have been found to be 2.21×10^3, 1.15×10^4 and 1.10×10^4 A cm^{-2}, respectively.[23] In total 0.1–10% Ho_2O_3-doped MgB_2 samples show no change in its crystal structure, T_c and H_{c2}, but exhibit significant enhancement in J_c and H_{irr}.[24] A similar study of RE oxide-doped MgB_2 samples, where RE oxides = La_2O_3, Nd_2O_3, Tb_4O_7, Er_2O_3, Lu_2O_3, has shown that the doping causes no change in T_c and does not lead to a serious decrease in J_c, despite the generation of larger amounts of impurity phases, such as RE borides and MgO.[22]

In the literature, there are very few studies on the doping effects of RE elements on the superconductivity of MgB_2. Therefore, more investigation needs to be done on doping MgB_2 with RE elements to find possible options for improving the superconducting performance of this compound. In this work, the doping effects of Er on the superconducting properties of porous MgB_2 have been studied.

2. Experimental

$(Mg_{1-x}Er_x)B_2$ samples with different stoichiometric ratios were prepared by the *in-situ* solid-state-reaction method. Commercially available high-purity powders of crystalline Mg (99.8%), Er (99.9%) and amorphous B (95–97%) were weighed to give a nominal composition of $(Mg_{1-x}Er_x)B_2$, where $x = 0.00$, 0.03 and 0.05. The mixtures of Mg, B and Er powders were thoroughly ground for 1 h in an agate mortar by hand in air. The mixtures, weighing about 2 g, were pressed into rectangular pellets 10×15 mm^2 in size under 1.3 GPa pressure. The pellets were put in a chrome tube and sintered at 650°C for 2 h under constant 10 bar Ar gas pressure. After the heat treatment, the chrome tube was cooled to room temperature by furnace cooling. Then, the second grinding process was performed. Finally, the obtained powders were pressed into the same rectangular pellet form under 1.3 GPa pressure and sintered at 750°C for 2 h under 10 bar Ar gas pressure, followed by furnace cooling to room temperature.

The phase compositions of the samples were determined from X-ray diffraction (XRD) patterns using a Rikagu D/Max-IIIC diffractometer with CuKα radiation, and the microstructures of the samples were analysed by a scanning electron microscope (SEM, JEOL JSM 6400). The upper critical field B_{c2} and the irreversibility field B_{irr} were defined as $B_{c2} = 0.9R(T_c)$ and $B_{irr} = 0.1R(T_c)$[25] from the resistance (R) *vs.* temperature (T) curves (5 mA ac) obtained by a four-probe resistivity measurements. Also, the T_c values were obtained from the resistivity curves of the samples. The magnetic properties (M–H loops) of the samples were determined using a vibrating sample magnetometre within the Quantum Design Physical Properties Measurement System for the temperature ranges from 4.2 to 35 K. The magnetic J_c (in A cm^{-2}) of the samples was calculated from the $M(H)$ curves *via* $J_c = 20\Delta M/[aV(1-a/3b)]$ on the basis of Bean's critical state model.[26] In this relationship, ΔM (in emu) is the width of the $M(H)$ hysteresis. V (in cm^3), a (in cm) and b (in cm) are the volume, length and width of the sample ($a < b$), respectively.

3. Results and discussion

Figure 1 shows the XRD patterns of the $(Mg_{1-x}Er_x)B_2$ ($x = 0.00$, 0.03 and 0.05) samples. It is very apparent from figure 1 that the undoped sample has the major phase of MgB_2, with a little amount of MgO. Also, it can be seen that the boride impurities ErB_4, ErB_2 and also an oxide phase Er_2O_3 have formed. As clearly seen from figure 1, the main peak belonging to MgB_2 at around 42.4° has decreased in intensity and has broadened for the doped samples. It is an indication of reducing the crystallite size for the doped samples. Table 1 also shows the variation of the lattice parameters of all samples. The lattice parameters a and c of the porous undoped sample are smaller than that of the dense MgB_2 reported in literature. The difference is possibly due to the porous structure of the undoped sample. It is well known that the lattice parameters of MgB_2 decrease with the increasing porosity.[27] Both the lattice parameters a and c increase with the increasing Er concentration, as given in table 1. It is expected from these results that some Er atoms have partially substituted into MgB_2, possibly at Mg sites.

The SEM images show the porous structure (the black area) and the agglomeration of particles in the undoped

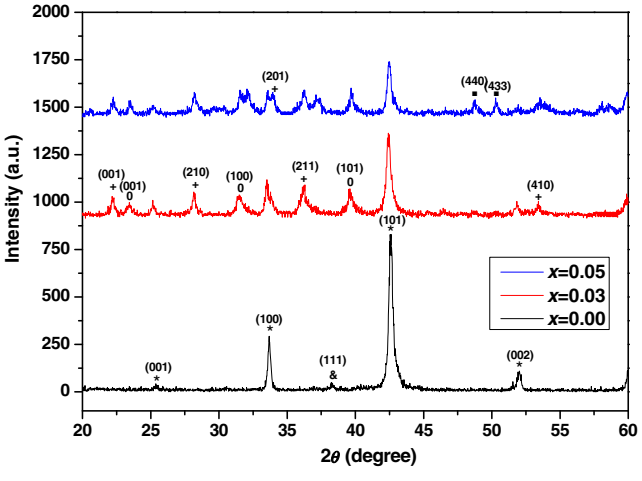

Figure 1. X-ray diffraction patterns for undoped and Er-doped MgB_2 samples. MgB_2 peaks are indicated with * symbol. Impurity peaks are indicated with the following symbols: & for MgO, ■ for Er_2O_3, + for ErB_4 and 0 for ErB_2, respectively.

Table 1. Data for Er-doped MgB_2 samples.

Samples	Lattice parameter, a (Å)	Lattice parameter, c (Å)	T_c^{onset} (K)	ΔT_c (K)	J_c (4.2 K, 3 T) (A cm^{-2})	J_c (15 K, 3 T) (A cm^{-2})	ρ (300 K) (μΩ cm)	ρ (40 K) (μΩ cm)	RRR	A_F
$x = 0.00$	3.073	3.511	38.63	1.97	2.2×10^3	0.6×10^3	1158.08	613.86	1.89	0.013
$x = 0.03$	3.074	3.523	38.49	0.67	1.1×10^5	6.2×10^4	249.07	103.09	2.42	0.050
$x = 0.05$	3.082	3.533	38.57	0.89	8.3×10^4	3.9×10^4	609.85	259.86	2.35	0.021

sample (see figure 2a). The porous structure decreases and the homogeneity increases with Er doping (see figure 2b and c). Also, it can be seen that the MgB_2 grains are smaller for the doped samples compared to the undoped one. It leads to an increase in the surface area of grain boundaries, which act as pinning centres in MgB_2.

Figure 3 shows the normal state resistivity *vs.* temperature measured at different applied magnetic fields up to 10 T for all samples over a temperature range of 10–300 K. The inset shows the resistivity *vs.* temperature curves at the temperatures between 10 and 45 K. It can be seen that the scattering in the undoped porous MgB_2 sample decreases with the increasing Er content. The resistivity at 40 and 300 K decreases from extraordinarily high value of 613.86 and 1158.08 μΩ cm, respectively, for the porous MgB_2, to 103.09 and 249.07 μΩ cm, respectively, for the 3 wt% Er-doped MgB_2 sample. Such high resistivity of the undoped sample can be a result of the presence of pores between the superconducting grains. As known, dense MgB_2-based materials have a significantly lower resistivity.[6] Hence, the relatively lower resistivity may be related to higher sample density and better inter-granular connectivity. In a polycrystalline bulk sample produced by hot press method at 700°C, the resistivity values are 2050 and 1560 μΩ cm at 300 and 50 K, respectively, as reported by Rogado *et al*[28] (the resistivity values have been taken from the small figures in Rogado *et al*[28]). Also, Sharma *et al*[29] have reported the T_c value of the MgB_2 sample, which was deliberately made with Mg deficiency, is to be around 39 K even as the resistivity at 300 K of the sample is above 100 mΩ cm. From these results, it can be said that the resistivity values of the doped and undoped samples are compatible with literature. The resistivity of 5 wt% Er-doped sample is higher than the resistivity of 3 wt% Er-doped sample. It is probably the result of the excess impurity phases. It can be seen from figure 3 that all samples show a sharp superconducting transition at around 38–39 K in zero field regime. However, the transition range becomes narrower for the doped samples. The T_c^{onset} and the ΔT_c values determined from figure 3 have been obtained to be 38.63, 38.49, 38.57 K and 1.97, 0.67, 0.89 K for 0, 3 and 5 wt% Er-doped samples, respectively (see table 1). The T_c^{onset} value of the undoped sample is acceptable, because in some high resistivity MgB_2 samples, it has been reported that T_c is surprisingly over 35 K.[30] Also, the minute suppression in T_c^{onset} values supports the partial substitution of Er into MgB_2 lattice. The narrower transition to superconductivity for the doped samples implies the improvement in homogeneity and

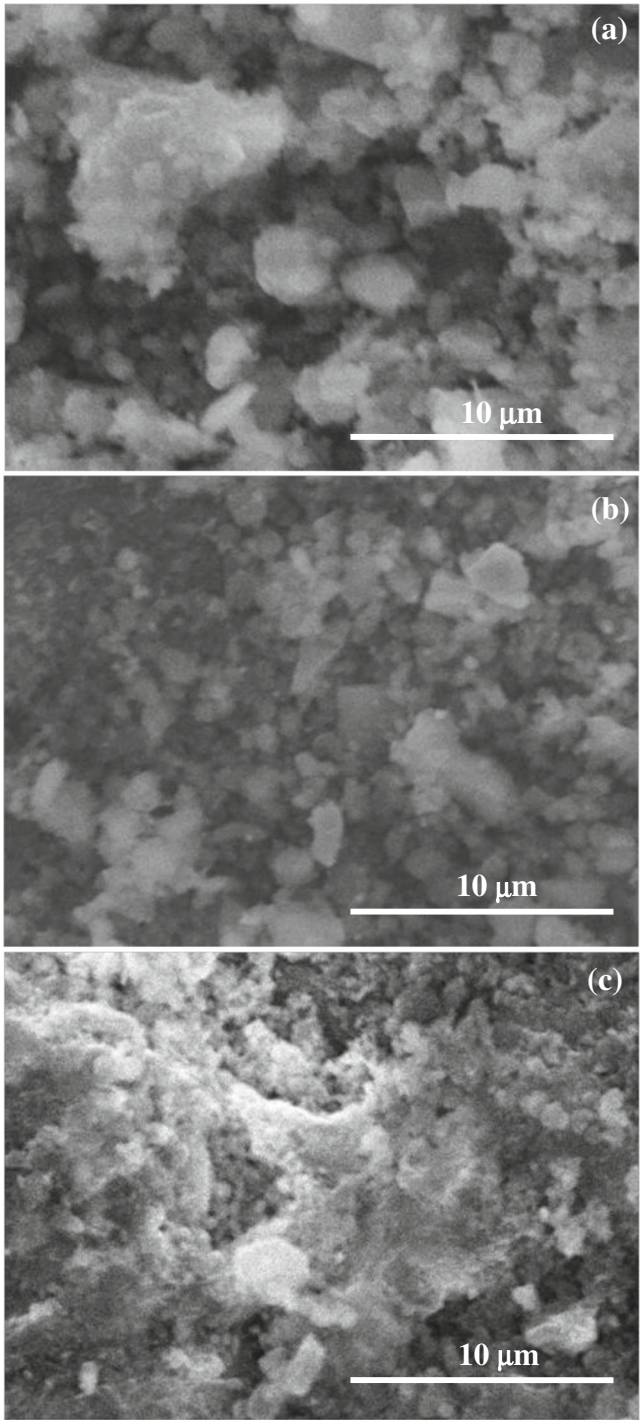

Figure 2. SEM images of (**a**) $x = 0.00$, (**b**) $x = 0.03$ and (**c**) $x = 0.05$ Er-doped MgB_2 samples.

grain connectivity. The transition temperatures of all samples decrease as usual with the increasing applied field, as seen from figure 3.

The residual resistivity ratios RRR related with the intragrain effect of grain boundary junctions have been calculated from the resistivity measurements (RRR = ρ(300 K)/ρ(40 K)). Also, the active area fractions (A_F) related with intergrain effect, have been evaluated by using the formula $A_F = \Delta\rho_{ideal}/[\rho(300\ K) - \rho(40\ K)]$. Here, $\Delta\rho_{ideal}$ is the ideal change in resistivity from 300 to 40 K for a fully connected sample, for which the value of 7.3 μΩ cm is typically used.[30,31] The residual resistivity ratios and the active area fractions for the undoped, 3 and 5 wt% Er-doped samples are 1.89, 2.42, 2.35 and 0.013, 0.050, 0.021, respectively, as shown in table 1. It is observed that the RRR and A_F values are higher for the doped samples than that of the undoped one. It is well known that the relatively high values of RRR indicate good quality of the samples. The fact that RRR shows an increasing trend is possibly due to the decrement of the grain sizes and the substitution of Er in MgB_2. The increase in A_F of the doped samples signals decreasing porosity, improving grain boundary and a better connectivity.

The temperature dependence of B_{c2} and B_{irr} for all samples is shown in figure 4. The B_{irr} and B_{c2} at various temperatures for the samples have been estimated from the resistive transition curves using the criteria of 0.1 and 0.9 of $\rho(B, T_c)$, respectively.[25] It is observed that the B_{c2} and B_{irr} values are significantly enhanced for the doped samples. The best B_{c2} and B_{irr} increments have been obtained for the 3 wt% Er-doped sample, because the slope of $dB_{c2}/d(T/T_c)$ for the 3 wt% Er-doped sample is larger compared to those for both the undoped and the 5 wt% Er-doped samples. For the best sample ($x = 0.03$) the B_{irr} value at 20 K reaches 9.7 T. It can be expected that the improvement in B_{irr} is because of the flux pinning induced by grain boundaries, which increase in the doped samples due to the suppression of grain growth. In addition, the reason of the increment in B_{c2} is probably the partial substitution of Er into MgB_2 crystal lattice.

The J_c characteristic of all samples have been estimated from the high field magnetization measurements $M(H)$, by invoking Bean's critical state model.[26] In this manner, the $J_c(B)$ results are plotted in figure 5 at the temperatures between 4.2 and 35 K. As seen from this figure, the J_c of the doped samples are higher than that of the undoped one for all fields and at all temperatures. The values of J_c at 4.2 K and under a field of 3 T have been calculated to be 2.2×10^3 A cm^{-2} for the undoped MgB_2 sample, 1.1×10^5 A cm^{-2} for 3 wt% Er-doped sample and 8.3×10^4 A cm^{-2} for 5 wt% Er-doped sample. The values of J_c under a field of 3 T and at the temperatures of 4.2 and 15 K have been listed in table 1. For the best sample ($x = 0.03$), at 15 K under a magnetic field of 4 T, the J_c value reaches 2.4×10^4 A cm^{-2}, which is higher than that of the undoped sample by an order of 10^3 (see figure 5). The J_c values show clearly that the Er-doped samples exhibit better current-carrying capabilities under external magnetic fields. This is an indication of the enhancement in the flux pinning strength of the doped samples. The J_c variation with the increasing Er content are compatible with the resistivity results (see table 1), as reported by Rowell[30] that an important implication of the high resistivity, if they are indeed due to limitations in the area of the sample that carries current, is that exactly the same limitations should apply to the sample area that carries supercurrent. It might be expected that the improvement in J_c of the doped samples is related with the depression on the growth rate of MgB_2 grains by Er doping and so, the increment in the surface area of the grain boundaries, which act as pinning centres in MgB_2. Also, the impurity phases can act as effective pinning centres in the doped samples.

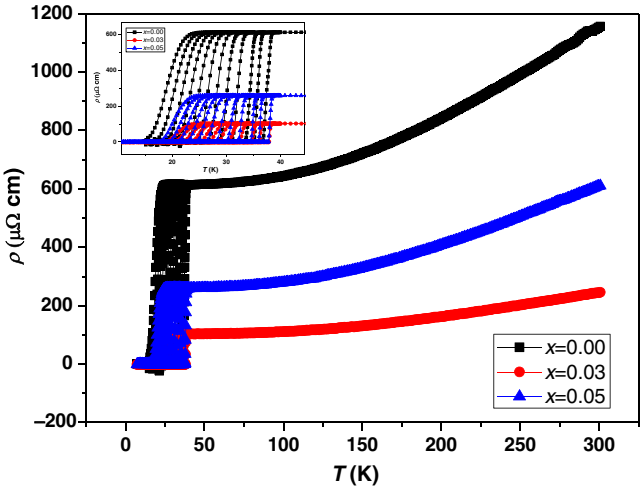

Figure 3. Superconducting transition zone resistivity *vs.* temperature from 10 to 300 K under different applied magnetic fields up to 10 T for undoped and Er-doped MgB_2 samples. The inset shows the resistivity at the temperatures between 10 and 45 K.

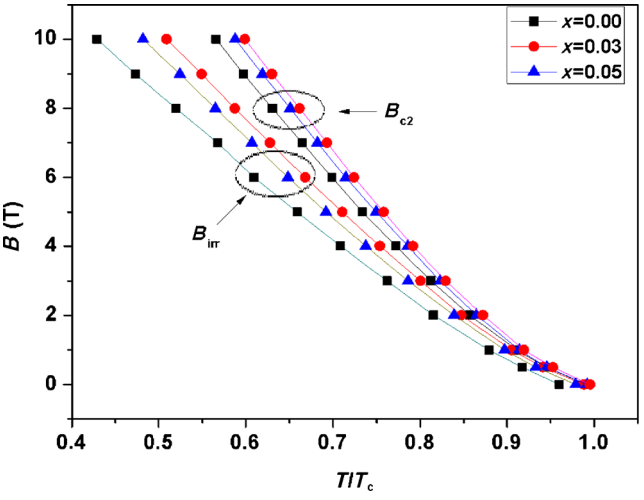

Figure 4. The upper critical field B_{c2} and the irreversibility field B_{irr} as functions of T/T_c for the samples synthesized with the nominal composition $(Mg_{1-x}Er_x)B_2$.

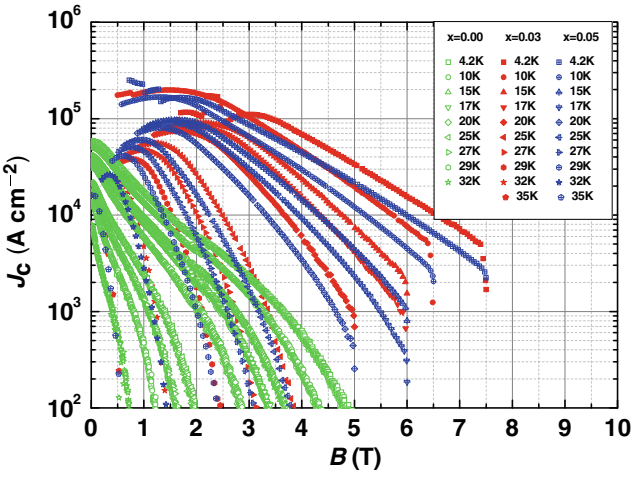

Figure 5. Magnetic field B dependence of the critical current density J_c for the undoped and Er-doped MgB_2 samples at the temperatures between 4.2 and 35 K.

4. Conclusions

In this study, the effects of Er doping on the superconducting properties of porous MgB_2 have been systematically studied. The B_{c2}, B_{irr} and J_c values are significantly enhanced for the doped samples, due to the degradation of porosity, the reduction in grain size and thus, the enhancement on grain connectivity and grain boundary pinning. Substantially enhanced B_{c2}, B_{irr} and J_c values have been observed in the 3 wt% Er-doped sample. It can be concluded from this experimental study that the RE element Er is an excellent candidate as a doping source for improving the superconducting properties of MgB_2, without significantly affecting the T_c of the material.

References

1. Nagamatsu J, Nakagawa N, Muranaka T, Zenitani Y and Akimitsu J 2001 *Nature* **410** 63
2. Kim H J, Kang W N, Choi E M, Kim M S, Kim K H P and Lee S I 2001 *Phys. Rev. Lett.* **87** 087002
3. Lyard L, Szabó P, Klein T, Marcus J, Marcenat C, Kim K H, Kang B W, Lee H S and Lee S I 2004 *Phys. Rev. Lett.* **92** 057001
4. Larbalestier D C *et al* 2001 *Nature* **410** 186
5. Liu C F, Yan G, Du S J, Xi W, Feng Y, Zhang P X, Wu X Z and Zhou L 2003 *Physica C* **386** 603
6. Putti M, Braccini V, Galleani E, Napoli F, Pallecchi I, Siri A S, Manfrinetti P and Palenzona A 2003 *Supercond. Sci. Technol.* **16** 188
7. Rowell J M, Xu S Y, Zeng X H, Pogrebnyakov A V, Li Q, Xi X X, Redwing J M, Tian W and Pan X 2003 *Appl. Phys. Lett.* **83** 102
8. Li H L, Ruan K O, Li S Y, Yu Y, Wang C Y and Cao L Z 2003 *Physica C* **386** 560
9. Yao C, Zhang X, Wang D, Gao Z, Wang L, Qi Y, Wang C, Ma Y, Awaji S and Watanabe K 2011 *Supercond. Sci. Technol.* **24** 055016
10. Bugoslavsky Y, Cohen L F, Perkins G K, Polichetti M, Tate T J, Gwilliam R and Caplin A D 2001 *Nature* **411** 561
11. Dou S X, Soltanian S, Horvat J, Wang X L, Zhou S H, Ionescu M, Liu H K, Munroe P and Tomsic M 2002 *Appl. Phys. Lett.* **81** 3419
12. Zhao Y, Feng Y, Cheng C H, Zhou L, Wu Y, Machi T, Fudamoto Y, Koshizuka N and Murakami M 2001 *Appl. Phys. Lett.* **79** 1154
13. Slusky J S *et al* 2001 *Nature (London)* **410** 343
14. Felner I 2001 *Physica C* **353** 11
15. Feng Y, Zhao Y, Sun Y P, Liu F C, Fu B Q, Zhou L, Cheng C H, Koshizuka N and Murakami M 2001 *Appl. Phys. Lett.* **79** 3893
16. Kuhberger M and Gritzner G 2002 *Physica C* **370** 39
17. Kitaguchi H and Kumakura H 2005 *Supercond. Sci. Technol.* **18** S284
18. Cheng C H, Zhao Y, Zhu X T, Nowotny J, Sorrell C C, Finlayson T and Zhang H 2003 *Physica C* **386** 588
19. Wang J, Bugoslavsky Y, Berenov A, Cowey L, Caplin A D, Cohen L F, Cooley L D, Song X and Larbalestier D C 2002 *Appl. Phys. Lett.* **81** 2026
20. Chen S K, Wei M and MacManus-Driscoll J L 2006 *Appl. Phys. Lett.* **88** 192512
21. Pan X F, Shen T M, Li G, Cheng C H and Zhao Y 2007 *Phys. Status Solidi (a)* **204** 1555
22. Katsura Y, Shimoyama J, Yamamoto A, Horii S and Kishio K 2007 *Physica C* **463–465** 225
23. Ojha N, Varma G D, Singh H K and Awana V P S 2009 *J. Appl. Phys.* **105** 07E315
24. Cheng C and Zhao Y 2006 *Appl. Phys. Lett.* **89** 252501
25. Hossain M S A, Kim J H, Xu X, Wang X L, Rindfleisch M, Tomic M, Sumption M D, Collings E W and Dou S X 2007 *Supercond. Sci. Technol.* **20** L51
26. Bean C P 1962 *Phys. Rev. Lett.* **8** 250
27. Grinenko V, Krasnoperov E P, Stoliarov V A, Bush A A and Mikhajlov B P 2006 *Solid State Commun.* **138** 461
28. Rogado N, Hayward M A, Regan K A, Wang Y, Ong N P, Zandbergen H W, Rowell J M and Cava R J 2002 *J. Appl. Phys.* **91** 274
29. Sharma P A, Hur N, Horibe Y, Chen C H, Kim B G, Guha S, Cieplak M Z and Cheong S W 2002 *Phys. Rev. Lett.* **89** 167003
30. Rowell J M 2003 *Supercond. Sci. Technol.* **16** R17
31. Jiang J, Senkowicz B J, Larbalestier D C and Hellstrom E E 2006 *Supercond. Sci. Technol.* **19** L33